Journal of Materials Chemistry B

Accepted Manuscript

ROYAL SOCIETY OF CHEMISTRY

www.rsc.org/materialsB

Journal Name

RSCPublishing

ARTICLE

Dual Use of Porphyrazines as Sensitizers and Viscosity Markers During Photodynamic Therapy

Cite this: DOI: 10.1039/xoxxoooooox

M. Angeles Izquierdo,[a] Aurimas Vyšniauskas,[a] Svetlana A. Lermontova,[b] Ilya S. Grigoryev,[b] Natalia Y. Shilyagina,[c] Irina V. Balalaeva,[c] Larisa G. Klapshina,[b, c*] Marina K. Kuimova[a*]

Received ooth January 2012,
Accepted ooth January 2012

DOI: 10.1039/xoxxoooooox

www.rsc.org/

Porphyrazines have recently emerged as a useful class of tetrapyrroles suitable for photodynamic therapy of cancer (PDT) with excellent uptake and retention properties *in vivo*. Here we demonstrate that the photophysical properties of cyano-phenyl porphyrazine **pz1** are strongly viscosity dependent, *i.e.* the fluorescence lifetime and the quantum yield of **pz1** increase as a function of solution viscosity. We have calibrated **pz1** as a red-emitting fluorescent 'molecular rotor' in a large range of viscosities from 80 to *ca* 5500 cP, in solutions of various solvent compositions and temperature. On the other hand, **pz1** works as an efficient PDT sensitiser, *i.e.* it induces apoptosis and necrosis in cells upon irradiation with red light through formation of singlet oxygen. We demonstrate that PDT in cells using **pz1** is accompanied by a significant viscosity increase by monitoring the fluorescence lifetime of the rotor. We suggest that this increase could be used as a completely new type of diagnostic and dosimetry tool during a PDT treatment.

Introduction

Viscosity is an important parameter determining the diffusion rate of species in condensed media. In biological systems, it can change as a consequence of disease, malfunction and cell death.[1-3] In the last decades, several fluorescence-based methods have been developed for probing diffusion on the microscopic scale, since they are minimally invasive and can be used to quantify small volumes of samples. Examples include fluorescence recovery after photobleaching,[4] fluorescence correlation spectroscopy,[5, 6] single particle tracking[7] and, more recently, molecular rotors.[8, 9]

Molecular rotors are a group of fluorophores in which fluorescence depends on the rate of intramolecular rotation. In media of high viscosity, intramolecular rotation is inhibited resulting in significant increases of the emission intensity and the fluorescence lifetime.[8] The development of ratiometric or fluorescence lifetime-based sensors is desirable, because they can be used in imaging experiments as concentration independent probes to monitor viscosity in heterogeneous systems such as cells, with organelles exhibiting a broad range of viscosity values.[10-15] Very importantly, dynamic imaging with molecular rotors allows to monitor viscosity changes upon perturbation, if the time scale of a change is slower than the time required for image acquisition. For example, we have previously reported changes in viscosity during light induced cell death in photodynamic therapy (PDT) of cancer, utilising a fluorescent molecular rotor, which allowed a concentration-independent ratiometric detection.[16]

While several molecular rotors of various structures are currently available, there is an active research effort into new viscosity-sensitive fluorophores.[12-14, 17] One desirable feature is intense absorption and emission of red light that can be useful *in vivo* to enable deep tissue penetration in the 'tissue optical window'.

Chart 1. Molecular structures of porphyrazines pz1-pz2

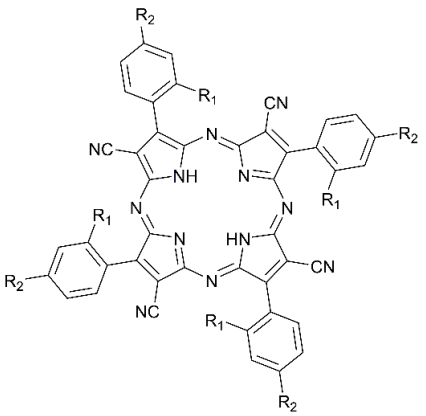

pz1 R_1 = H, R_2 = F
pz2 R_1 = CH_3, R_2 = H

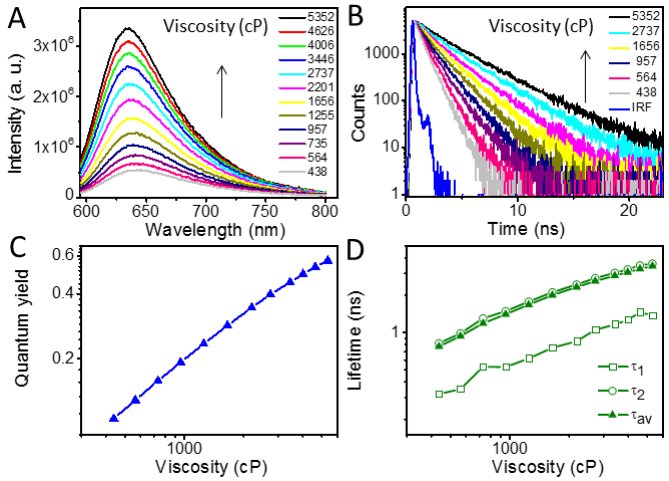

Fig. 1. Fluorescence characterisation of **pz1** in glycerol at varied temperatures (4 – 36 °C). (A) Fluorescence spectra. (B) Time resolved fluorescence decays (C) Fluorescence quantum yield *vs* viscosity. (D) Lifetimes (τ_1, τ_2, τ_{av}) *vs* viscosity.

Porphyrazines have recently emerged as a very important class of tetrapyrroles suitable for PDT with excellent uptake and retention properties *in vivo*.[18, 19] PDT is a clinical treatment for several types of cancer and relies on the excitation of a photoactive drug, which subsequently produces short-lived cytotoxic species, such as singlet oxygen.[20]

One of the important challenges in PDT is the correct light dosimetry, to achieve the most favourable treatment outcome.[21-28] Herein, we report a new red-emitting viscosity-sensitive molecular rotor **pz1** (Chart 1) that is suitable for quantitative measurements of viscosity in a large dynamic range. We also demonstrate a new approach to the PDT dosimetry, based on fluorescence lifetime measurements of **pz1**. PDT in cells using **pz1** is accompanied by cell death and a significant viscosity change, as measured by its fluorescence lifetime. Thus we demonstrate that photoinduced changes in viscosity could be used as a new diagnostic tool during PDT treatments and could be indicative of the treatment outcome.

Results and discussion

Photophysical characterization in solution

In order to explore the potential use of **pz1** as a viscosity marker, the photophysical properties were first studied in different solvents in a wide range of viscosities and polarities (Table S1, Figs. S1A and 1B; ESI). The absorption and emission maxima (*ca* 580 and 640 nm, respectively) are polarity dependent and shift bathochromically as the polarity decreases, see ESI. We note that the quantum yields of **pz1** are less than 0.02 in low viscosity media, regardless of the polarity of the solvent. Only in viscous media, such as glycerol, concentrated aqueous sucrose solutions and castor oil, the compound is highly fluorescent.

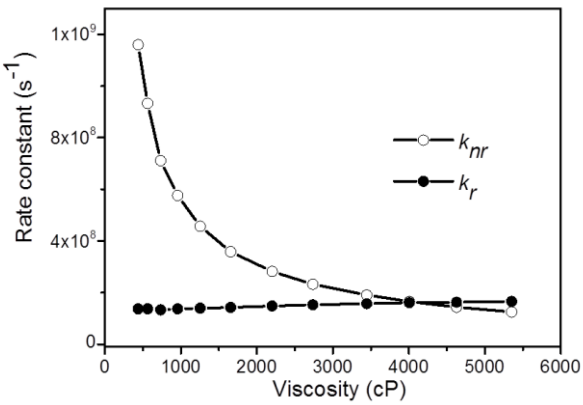

Fig. 2. Radiative and non-radiative constants plotted against the viscosity.

To investigate how the fluorescence properties of **pz1** depend on viscosity we have recorded fluorescence spectra and time resolved fluorescence decays in solutions of a large range of viscosities ranging from 1 cP to 5360 cP. First, a spectroscopic study of **pz1** was carried out in glycerol at temperatures ranging from 36 ºC to 4 ºC, which corresponds to a viscosity range between 5360 cP and 440 cP, Fig. 1. The UV-visible absorption spectra of **pz1** are independent of viscosity and temperature (Fig. S1C; ESI). The shape and maximum wavelength of the emission spectra also do not change. However, a marked increase in the fluorescence intensity is observed upon the viscosity increase. The quantum yield *vs* viscosity graph conforms to the Förster-Hoffmann Equation 1,[29] where z and α are constants, η is viscosity (Fig. 1C). Notably, viscosity also correlates with the fluorescence lifetime (τ_f) according to Equation 2,[8] Fig. 1B.

The decays of **pz1** were fitted to a biexponential model and the values of both lifetimes were found to increase with the viscosity of the media (Fig. 1D).

$$\Phi_f = z\eta^{\alpha} \qquad \text{(Equation 1)}$$

$$\tau_f = z k_r^{-1} \eta^{\alpha} \qquad \text{(Equation 2)}$$

To confirm that **pz1** indeed works as a molecular rotor we calculated the radiative (k_r) and the non-radiative rate constants (k_{nr}), based on the quantum yield and the average lifetime values (τ_{av}) and the results are shown in Fig. 2. As viscosity increases up to 4000 cP, k_r remains constant while k_{nr} decreases sharply. Thus, the increase in the fluorescence intensity and the lifetime with increasing viscosity must be due to the suppression of non-radiative processes, such as intramolecular rotation.[8, 9] In the example above, we have achieved the change in viscosity by changing the temperature, however, similar results were also obtained in various mixtures of methanol/glycerol performed at a fixed temperature (Fig. S2; ESI). Overall, our results are consistent with **pz1** acting as a molecular rotor, that works in a wide viscosity range. **Pz1**

represents one of the most red emitting lifetime-based molecular rotors reported to date, which is a useful feature that allows to achieve deeper tissue penetration, due to a good overlap with the 'tissue optical window'.

Since **pz1** is a new molecular rotor that is based on a previously unexplored molecular structure, we have synthesised a derivative **pz2** (Scheme 1, ESI) to investigate the possible mechanism of the intramolecular non-radiative decay. The presence of the *ortho*-methyl group in **pz2** was expected to hinder the rotation of the C-C bond between the tetrapyrrole macrocycle and the phenyl unit. The photophysical properties of **pz2** were measured in glycerol, castor oil and methanol and are shown in Table S1 and Fig. S3 (ESI). The absorption and emission bands of **pz2** are similarly positioned to the bands of compound **pz1**, but the quantum yield in glycerol at room temperature is 0.39, 1.4× higher than the quantum yield of **pz1** under the same experimental conditions. The fluorescence decays of **pz2**, which are biexponential, are characterised by longer lifetimes, suggesting that the rotation of the phenyl unit plays an important role in the molecular rotor properties of **pz1** core.

In order to compare the sensitivity of **pz1** and **pz2** to viscosity, the calibration curve was obtained for **pz2** in glycerol as a function of temperature in the same range of viscosities as determined for **pz1** (Fig. 3). The corresponding plots for **pz2**, according to the logarithmic form of the Förster Hoffmann Equation (Equation 3),[8] show a shallower slope, again confirming that the function of **pz2** as a molecular rotor is restricted due to the presence of the methyl substituent on the phenyl group. A similar trend was observed when comparing **pz2** to a control molecule related to **pz1**, but without the fluoride group in the *para* position of the phenyl substituent (data not shown). This resembles the function of the molecular rotor Bodipy-meso-phenyl, where the rotation of the phenyl group in the meso-position (as well as its function as a molecular rotor) was eliminated by introducing *ortho*-methyl substituents to the phenyl group.[10] However, the possible electronic effect of the *para* fluoride substituent on the photophysics of **pz1** can not be ruled out.

While **pz2** also acts as a molecular rotor, it is clearly less sensitive to changes in viscosity and therefore **pz1** was used in all subsequent experiments.

$$\log\tau_f = \alpha\log\eta + \log\left(\frac{z}{k_r}\right) \qquad \text{(Equation 3)}$$

Calibration curves

To ensure the most complete calibration of **pz1**, we have measured the fluorescence quantum yield and fluorescence lifetimes in solutions of methanol/glycerol of different compositions and at different temperatures.

The calibration curves obtained for three different mixtures of glycerol/MeOH (from 70 to 90% glycerol) and pure glycerol recorded at temperatures between -2 °C and 36 °C exhibit a strong response to viscosity up to 5360 cP (Fig. S4; ESI). The curves $\tau_f = f(\eta)$ obtained in all four solvents follow a similar trend, with a small deviation which could be due to temperature or polarity effects. The close overlap of all four traces allows us to rule out temperature as the main effect on the k_{nr} and assign the changes in k_{nr}, Fig. 2, to the effect of viscosity.

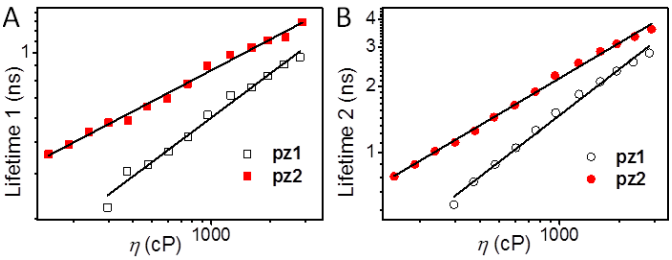

Fig. 3. Calibration graph of τ *vs* η according to Equation (3) in glycerol for **pz1** and **pz2**. (A) τ_1 *vs* η ; (B) τ_2 *vs* η.

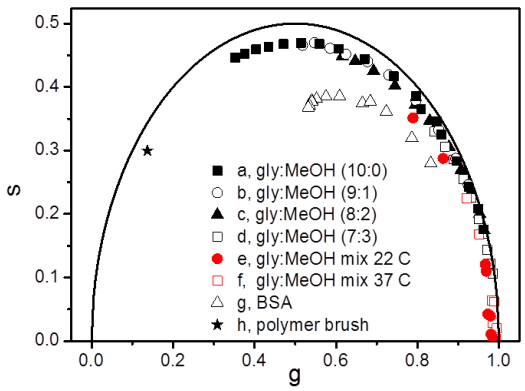

Fig. 4. Phasor plot of TCPSC (black, λ_{exc} = 635 nm) and FLIM (red, λ_{exc} = 800 nm) data of **pz1** recorded in different media (see Fig. key): a) glycerol at varied temperatures 4 – 36 °C; b) glycerol: MeOH (9:1) at varied temperatures 4 – 29 °C; c) glycerol: MeOH (8:2) at varied temperatures -2 – 25°C; d) glycerol: MeOH (7:3) at varied temperatures -2 – 22°C; e) glycerol/MeOH mixtures at 37°C, containing 70 – 100 % glycerol; f) glycerol:MeOH mixtures at 22 °C, containing 70 – 100 % glycerol g) different concentrations of BSA, from 0.12 to 5.03 equivalent, h) a polymer brush.

Phasor analysis of solution data

Noting that the fluorescence decays of **pz1** are biexponential we have used the phasor approach to analyse the data (see experimental section). Phasors provide a model free approach for visualizing heterogeneity in time-resolved fluorescence data.[30] In addition, in the phasor approach trends are easy to see upon visual inspection of the phasors of data,[31] which will be extremely useful when analyzing variability in Fluorescence Lifetime Imaging Microscopy (FLIM) data upon photoinduced cell death. In a phasor approach, the real component, *s(ω)*, of a Fourier transform of the decay is plotted *vs* the imaginary component *g(ω)*. Each decay is identified by their position

relative to the universal circle, a circle centred at (0, ½) in the coordinates above, with a radius of 1/2. The monoexponential decays lie on the circle while the biexponential decays lie on the secant connecting two individual decay components.

The phasor plot of the decays of **pz1** recorded in different mixtures of glycerol/MeOH as a function of temperature is shown in Fig. 4. As noted previously, a good overlay is observed for the different mixtures of the same viscosity. As the viscosity increases, a deviation of phasors from the universal circle is observed, highlighting a more pronounced biexponential nature of these decays.

We have developed a method to quantify the unknown viscosity of a phasor point lying on or near the universal circle, by measuring an angle between the *g* axis and a secant between the centre of the universal circle and the point of interest (see Fig. S5; ESI). This approach, which we termed 'angle phasor representation', will be useful when quantitatively interpreting the phasor data of **pz1** binding to proteins or when in cells.

Interaction with macromolecules

When inside a cell, it is likely that **pz1** will interact with various bio- or macro-molecules. To examine the effect such interaction might have on the spectroscopic properties of **pz1**, we recorded the fluorescence spectra and decays of **pz1** in liposomes, in aqueous solution upon interaction with bovine serum albumin (BSA) and in a rigid polymer that is known to effectively solubilise **pz1**[32] (Table S2; ESI).

Liposomes are a convenient model system to mimic lipid membranes.[33, 34] The absorption and emission spectra of **pz1** were measured in aqueous suspensions of liposomes, when incorporated in two types of lipid coatings, L-α- lecithin and 1,2-dioleyl-sn-glycero-3-phosphocholine (DOPC). The absorption and emission maxima are very similar in both samples (Table S2; ESI). These values (λ_{abs} = 592 – 596 nm and λ_{em} = 634 – 639 nm) are very close to those observed in polar solvents and in glycerol (λ_{abs} = 593 nm and λ_{em} = 635 nm) (Table S1, ESI) and indicate that **pz1** is located in a relative polar environment, rather than in a non-polar lipid tail region of the bilayer. The localization of **pz1** near the non-viscous interface of water-lipid heads is further confirmed by short fluorescence decays observed in both liposome systems (Table S2; ESI). From these data we conclude that **pz1** is not likely to incorporate inside lipid bilayers in cells.

Considering the propensity of organic dyes to associate with proteins[35] we have recorded the decays of **pz1** in the presence of varying concentrations of BSA. In the presence of BSA a significant increase in the quantum yield and the fluorescence lifetime is observed, indicating that the interaction of **pz1** with BSA does indeed take place. A significant blue shift in the absorption and the emission spectra is observed upon increasing BSA concentration (Table S2; ESI). This large blue shift and the phasors that are situated inside the universal circle, Fig. 4, set the BSA data apart from every other dataset obtained for **pz1**. We hypothesise that in the presence of BSA, the structural flexibility of **pz1** is reduced due to binding. Based on this data, we also hypothesise that upon increasing concentration of BSA in solution, two modes of binding of **pz1** and BSA might occur, see Fig. S10, ESI.

Finally, we have investigated the behaviour of **pz1** in the presence of amphiphilic polyimide brushes, as a model for complete immobilization of the molecular rotor. Previously, these brushes were used as solubilizers and nanocontainers for delivery of **pz1** *in vitro*.[32] The absorption and emission spectra of **pz1** in polymer brush exhibit maxima at 597 nm and 639 nm, respectively, and a dramatic increase in the quantum yield, to 0.54, the highest value observed in any solvent system investigated so far at room temperature. Importantly, fitting the decay traces to a biexponential function reveals a very long fluorescence lifetime of 6.91 ns (96% contribution), indicating that **pz1** is located in a very rigid media, where intramolecular rotation is strongly hindered. The decay collected for **pz1** for the polymer brush is included in the phasor plot, Fig. 4. This point is located close to the semicircle, as expected from its almost monoexponential decay and follows the trend of the calibration data, providing the phasor value which we will assume to be close to complete immobilisation of **pz1**. Thus we believe that the phasor approach allows an easy calibration of the observed lifetime data.

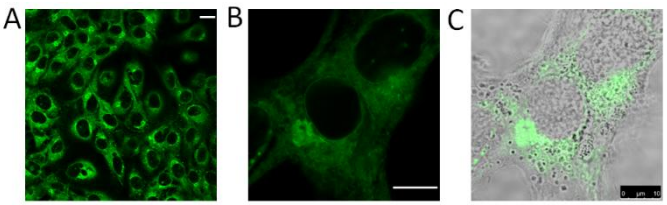

Fig. 5. Confocal images of SK-OV-3 cells recorded following incubation of a layer of live cells with 4 μM solution of **pz1** in HBSS for 30 minutes. (A, B) Fluorescence images at different magnification (λ_{exc} = 561 nm, λ_{em} = 600 – 800 nm). (C) Composite images of fluorescence and white light transmission. Scale bar is 20 μm in A and 10 μm in B and C.

Microscopic characterization

Cell staining experiments were carried out in SK-OV-3 cells using different incubation concentrations of **pz1** at 37° C. The working concentration was fixed between 2 – 4 μM, which allowed good count rate and did not have any negative effect on the cell viability (Figure S6, ESI). Confocal images reveal a good cellular uptake for the dye and a remarkable increase in the fluorescence signal of the dye in cells (Fig. 5), as compared to the weak signal observed in low viscosity solutions (0.37 – 2 cP, Table S1, ESI) and in the cell incubation media (1 cP). These results indicate that **pz1** is located in an environment with restricted mobility within cells. However, fluorescence intensity values are concentration dependent and cannot be used to monitor viscosity in heterogeneous systems.

In order to obtain concentration independent microscopic data, FLIM images were obtained from SK-OV-3 cells incubated with porphyrazine **pz1,** Fig. 6. The data can be fitted with a biexponential function with a good χ^2 (Fig. 6F). The lifetime histograms of τ_1 and τ_2 are of a nearly Gaussian shape, with the

maximum at 0.23 ns and 1.22 ns, respectively (Figs. 6A and 6B, left panels). The relative contribution histograms of α_1 and α_2 are of a nearly Gaussian shape as well, with the maximum at 0.89 and 0.11, respectively (Figs. 6B and 6D, left panels). While the same decay model is appropriate for the fitting of both the calibration datasets and in cells, it is immediately obvious that the parameters from these two fits are different. Thus, the amplitude of the shorter decay component τ_1 is *ca* 90% in cells, while it was shown to be 20% in model mixtures of 100-5000 cP (Fig. S4; ESI). However, at low viscosity the calibration data show τ_1 as low as 40-50%.

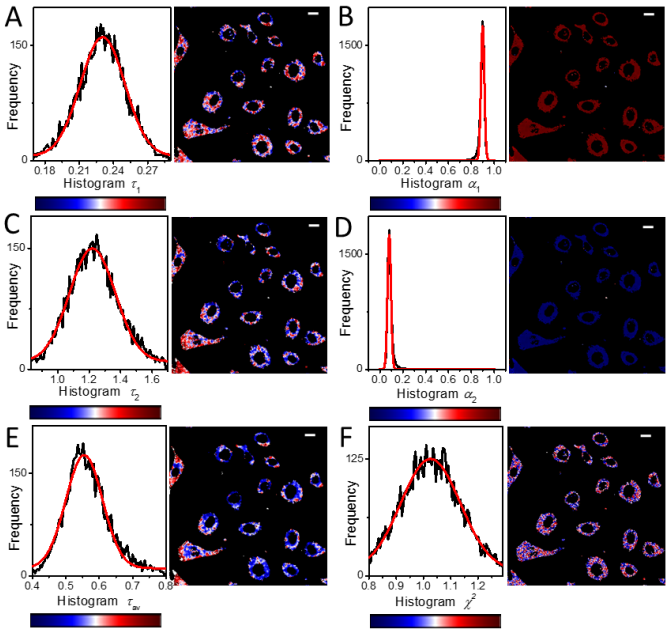

Fig. 6. FLIM histograms (left panels) and FLIM images (right panels) of SK-OV-3 cells incubated with 4 μM solution of **pz1** obtained following 800 nm pulsed excitation and (600 – 750) nm fluorescence detection. A seismic colour scale used to assign the lifetimes (A) τ_1, (C) τ_2 and (E) τ_{av}; the relative contributions (B) α_1 and (D) α_2 and (F) the χ^2 in the corresponding images.

It is also noteworthy, that no direct correlation is observed between the **pz1** decays in cells and the BSA binding data, either at low or high BSA concentrations. In summary, we cannot simply use the calibration dataset to determine the viscosity of the **pz1** microenvironment in cells. However, the overall imaging experiments reveal a remarkable increase in the fluorescence signal and lifetime of **pz1** in cells as compared to the weak signal observed in low viscosity solutions. These results indicate that **pz1** is located in a microenvironment of restricted mobility and it could be potentially used to monitor processes associated with changes in the local rigidity of the media, such as photoinduced cell death during PDT.

PDT dosimetry

Tetrapyrrol macrocycles, such as porphyrins and porphyrazines, are well established as photosensitisers in PDT.[20, 36-39] We investigated the potential use of the compound **pz1** as PDT sensitizer in SK-OV-3 cells. Selective irradiation of cells loaded with **pz1** resulted in dose dependent loss of cell culture viability (Fig. S6, ESI) and dramatic morphological changes, including cell contraction and detachment along with blebbing and bubble formation were observed in confocal experiments (Fig. S7; ESI). Cell death was confirmed by SYTOX® green nucleic acid stain that penetrates cells with a compromised plasma membrane (Figs. 7A and 7B). Viability control experiments in the absence of photosensitizer show that cells loaded with Rhodamine 123 exhibit the fluorescence characteristic of viable mitochondria after irradiation, confirming that the observed phototoxicity is due to the presence of **pz1** in cells (Fig. S8; ESI).

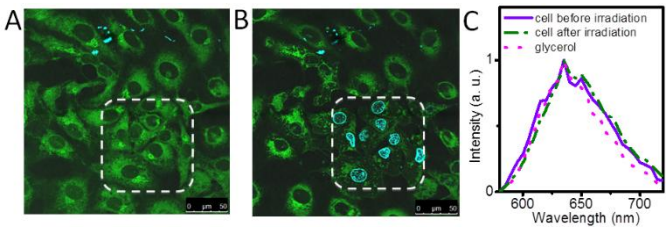

Fig. 7. (A, B) Sequential acquisition of fluorescence confocal images of SK-OV-3 cells incubated with 4 μM solution of **pz1** (λ_{exc} = 561 nm, λ_{em} = 650 – 759 nm) and 1 μM solution of SYTOX® green nucleic acid stain (λ_{exc} = 488 nm, λ_{em} = 500 – 530 nm). (A) Before and (B) 15 min after selective irradiation at λ_{exc} = 561 nm of the cells included within the dashed rectangle. Scale bar 50 μM. (C) Normalized fluorescence spectra of **pz1** in cells before and after irradiation and in glycerol (λ_{exc} = 561 nm, em 590 – 785 nm, 10 nm detection bandwidth, 5 nm detection step).

The emission spectra of **pz1** in cells were recorded before and after irradiation (Fig. 7C) and are similar to the emission spectrum of **pz1** in glycerol. All spectra were recorded on the same microscope setup to avoid errors associated with different detector sensitivities. The shape and the position of the spectra are identical in cells and in glycerol and the **pz1** spectrum in cells does not change upon irradiation (Fig. 7C). No blue shift is observed for **pz1** in cells with respect to glycerol, giving evidence against the surface-binding scenario as was observed in the BSA experiments. However, other types of binding cannot be excluded.

The data above demonstrate that **pz1** has two important functions: it is simultaneously a PDT photosensitiser and a molecular rotor that can measure viscosity. Only one previous example of such dual function has been reported, a conjugated porphyrin dimer that measured viscosity *via* ratiometric spectral detection.[40] It was previously demonstrated using the above compound that intracellular viscosity increases dramatically during photoinduced cell death.[16]

We have investigated the applicability of **pz1** for real time monitoring of photo-induced dynamic changes in viscosity during PDT using FLIM. SK-OV-3 cells were irradiated at 561 nm every 3 minutes and FLIM images acquired consecutively after each irradiation reveal a significant irradiation-dependent

increase in the fluorescence lifetimes of the dye (Figs. 8 A-C). These results are in agreement with previous data in cells obtained using a conjugated porphyrin dimer as a ratiometric molecular rotor.[16]

The plot of fluorescence lifetime of **pz1** *vs* the irradiation time reveals that the most significant changes in the lifetime take place during the first 6 min of irradiation (Figs. 8D, E), after which the increase is no longer noticeable. A change in the amplitude of two populations (lifetime components) of **pz1** is also observed, both factors indicating a change in the rigidity of the media. We again confirmed by SYTOX green staining that the cells irradiated in the FLIM experiment are permeable to SYTOX green stain after 6 min of irradiation (Fig. S9, ESI). The above results indicate that the increase in fluorescence lifetime of **pz1** with irradiation can be useful as a new dosimetry tool for monitoring the progress of PDT treatment, by linking the marked increase in viscosity upon irradiation to cell death.

PDT is a clinically relevant treatment modality, which is currently used for a range of neoplastic conditions. However, PDT dosimetry remains one of the important challenges, with physical properties of the tissue, light source placement for the relevant measurement and uncertainties in tissue oxygenation strongly affecting dosimetry measurements *in vivo*. On a single cell level, attempts to quantify singlet oxygen required for cell death have been made, but the quantification is restricted to the extracellular space at best.[27] We believe that detecting molecular rotor fluorescence can become a new unique approach to PDT dosimetry, utilising the phenomenon of structural changes on the cellular level of tissues subjected to PDT.

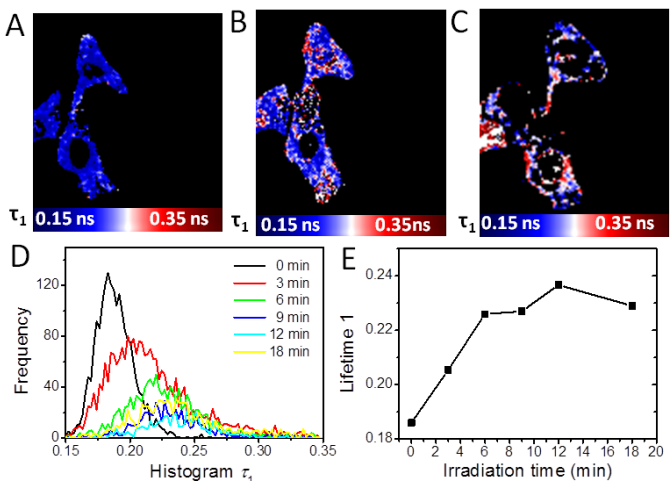

Fig. 8. (A-C) FLIM images of SK-OV-3 cells incubated with 4 μM solution of **pz1** for 30 min (λ_{exc} = 800 nm, λ_{em} = 600 – 750 nm). (A) Before, (B) after 3 min and (C) after 18 min irradiation (λ_{exc} = 561). (D) FLIM histogram of τ_1 obtained after different irradiation times. (E) Plot of τ_1 *vs* irradiation time.

The mechanism of the viscosity increase upon irradiation

The FLIM data of SK-OV-3 cells incubated with **pz1** before and after initial irradiation (Figs. 9 A-C) were analysed using the phasor approach (Figs. 9 D-F) in order to simplify the analysis of FLIM images. Fig. 9D shows the specific clustering of points in the phasor plot corresponding to the FLIM data of **pz1** in cells before irradiation. In this case, the phasor does not lie on the universal circle, consistent with the fact that a complex decay was detected in the classical FLIM analysis, Fig. 6. Figs. 9E and 9F show the appearance of an additional clustering of points, corresponding to cells that have been irradiated and changed their environment markedly, as detected by **pz1**. The second phasor cloud corresponding to the irradiated cells lies further to the top and left of the universal circle consistent with the increased average lifetime (and effective viscosity) of these cells. It should be noted that the phasor cloud of irradiated cells exhibits a very well defined cluster of data points, indicating that the FLIM data of individual cells result in similar values after irradiation. This was further confirmed by comparison of the τ_{av} FLIM histograms of the individual irradiated cells from Fig. 9C.

It is interesting to note that the phasors of healthy and irradiated cells appear to lie on the straight line connecting two points of the universal circle, characterised by the viscosities of 51 cP and > 5000 cP. Continuous irradiation leading to PDT causes a progressive shift upwards and left on a secant connecting these two viscosity points, Fig. 9G. This is consistent with a gradual change in % abundance of the population of each of these environments. Thus, it appears that PDT with **pz1** creates high viscosity environments (viscosity of *ca* 5000 cP) and depletes lower viscosity environments (viscosity of *ca* 50 cP), rather than causes a continuous change in viscosity. Such level of detail was not accessible with ratiometric analysis of viscosity increase during PDT, reported previously.[16]

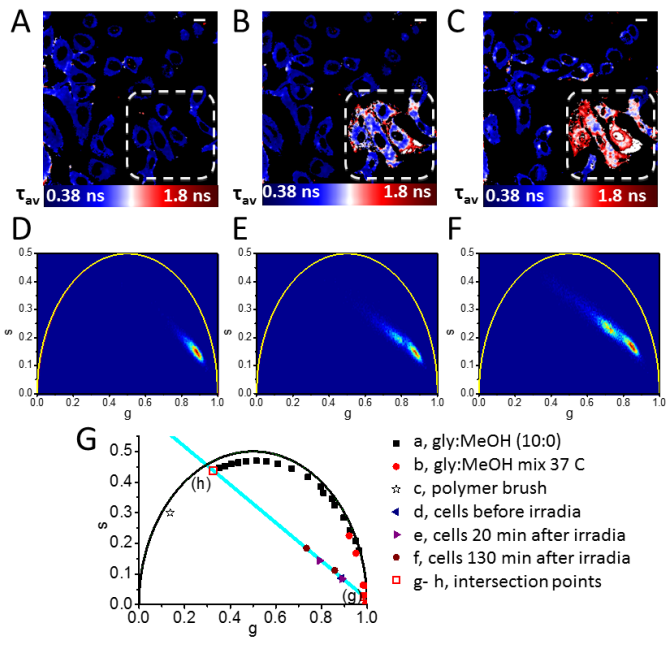

Fig. 9. (A-C) FLIM images and (D-F) phasor plots of SK-OV-3 cells incubated with 4 μM solution of **pz1** obtained following

800 nm pulsed excitation and (600-750) nm fluorescence detection. (A, D) Before and (B, E) 20 min and (C, F) 130 min after selective irradiation of the cells included within the dashed rectangle (irradiation conditions λ_{exc} = 561 nm, 5 min). A seismic colour scale is used to assign the lifetimes in the FLIM images. (G) Phasor plot including (a) calibrations of **pz1** in glycerol at varied temperatures, (b) calibrations of **pz1** in glycerol:MeOH at 37 °C, (c) a polymer brush, (d-f) the centroids of the clustering of points corresponding to graphs D-F, (g-h) intersection points corresponding to viscosities of 51 cP and > 5000 cP. Scale bar is 20 μm.

It is noteworthy that the initial viscosity of *ca* 50 cP measured here is similar to 80 cP measured by ratiometric molecular rotor based on the conjugated porphyrin dimer structure inside SK-OV-3 cells before PDT.[16] The second type of the environment that is apparently created by PDT is very rigid. However, we note that **pz1** is not completely immobile there, as the lifetime value is significantly lower than for **pz1** in a polymer brush (6.9 ns; shown by a star sign on Fig. 9G) or the binding scenario in the case of BSA (Fig. S10; ESI). Likewise, an increase in the contribution of a rigid-type environment upon irradiation seems inconsistent with binding. Alternatively, a shorter fluorescence decay component of **pz1** in healthy cells might be due to quenching, which could be alleviated to a certain extent upon PDT, causing a lifetime increase. Overall, our results indicate that the phasor plot representation is a simple and convenient tool for monitoring microenvironmental changes associated to photoinduced cell death during PDT. At the same time, the level of detail available from the lifetime analysis is considerably greater than what was possible with the ratiometric analysis which cannot distinguish between two species of different 'viscosity' in the same diffraction (or acquisition) limited pixel.

In order to investigate the mechanism of photoinduced viscosity increase. SK-OV-3 cells incubated with **pz1** were irradiated in the presence of NaN_3, a well known quencher of singlet oxygen that works intracellularly.[41, 42] The confocal and FLIM images obtained during irradiation in the presence of NaN_3 are shown in Fig. S11 (ESI) and show no irradiation-induced changes. These results suggest that the observed increase in viscosity observed in the presence of **pz1** is mediated by singlet oxygen and probably involved singlet oxygen-induced crosslinking, which is also consistent with the large viscosity increase upon irradiation. We hypothesise that it is indeed the cross links that create an extremely rigid environment for **pz1**, characterised by a viscosity of 5000 cP.

Conclusions

Here we presented a new molecular rotor **pz1** which works as an excellent dual agent, allowing a simultaneous PDT treatment and the monitoring of its progress and the mechanism by fluorescence lifetime imaging. The phasor analysis of FLIM data allowed us to detect at least two domains of high viscosity in cells, of 50 and 5000 cP, and the formation of the latter was promoted by PDT. While the main focus of this study was to improve our fundamental understanding of the light induced processes in the irradiated cell, we also believe that these results can have practical significance to PDT treatment of cancer. Further research is required to elucidate exact links between viscosity in individual cells and the mechanism of lesion death (*i.e.* apoptosis and necrosis). As such, compound **pz1** is currently being tested *in vivo* in mice cancer models.

Acknowledgements

MKK is thankful to the EPSRC for the Career Acceleration Fellowships. This work was partially supported by the European Commission in the form of Marie Curie individual Fellowship to MAI. AV thanks the EPSRC for the Prize Studentship. LGK is thankful to the Ministry of Education and Science of Russian Federation grant (Contract 14.Z50.31.0022). LGK and IVB are thankful to the Russian Foundation for Basic Research (RFBR, Contract 13-04-40228-H). We are thankful to Prof AV Yakimansky for donating the sample of polymer brushes studied previously.32 We are thankful to the Royal Society Exchanges (UK) – RFBR (Russia) joint grant to MKK and LGK for facilitating bilateral visits.

Notes and references

[a] Department of Chemistry, Imperial College London, Exhibition Road, London SW7 2AZ, United Kingdom, E-mail: m.kuimova@imperial.ac.uk
[b] Institute of Organometallic Chemistry of the RAS, Nizhny Novgorod, Russia, E-mail: klarisa@iomc.ras.ru
[c] Lobachevsky State University of Nizhny Novgorod, Nizhny Novgorod, Russia

Electronic Supplementary Information (ESI) available: Synthesis and characterization of compound **pz2**. Additional spectroscopic and imaging data. See DOI: 10.1039/b000000x/

1. M. Shinitzky, *Physiology of membrane fluidity*, CRC Press, Boca Raton, 1984.
2. G. Deliconstantinos, V. Villiotou and J. C. Stavrides, *Biochemical Pharmacology*, 1995, **49**, 1589-1600.
3. G. S. Zubenko, U. Kopp, T. Seto and L. L. Firestone, *Psychopharmacology*, 1999, **145**, 175-180.
4. M. J. Dayel, E. F. Y. Hom and A. S. Verkman, *Biophys. J.*, 1999, **76**, 2843-2851.
5. J. Korlach, P. Schwille, W. W. Webb and G. W. Feigenson, *Proc. Natl. Acad. Sci. U. S. A.*, 1999, **96**, 8461-8466.
6. N. L. Thompson, A. M. Lieto and N. W. Allen, *Curr. Opin. Struct. Biol.*, 2002, **12**, 634-641.
7. R. Iino and A. Kusumi, *J. Fluoresc.*, 2001, **11**, 187-195.
8. M. K. Kuimova, *Phys. Chem. Chem. Phys.*, 2012, **14**, 12671-12686.
9. M. A. Haidekker and E. A. Theodorakis, *Org. Biomol. Chem.*, 2007, **5**, 1669-1678.
10. M. K. Kuimova, G. Yahioglu, J. A. Levitt and K. Suhling, *J. Am. Chem. Soc.*, 2008, **130**, 6672-6673.
11. J. A. Levitt, M. K. Kuimova, G. Yahioglu, P. H. Chung, K. Suhling and D. Phillips, *J. Phys. Chem. C*, 2009, **113**, 11634-11642.
12. I. López-Duarte, T. T. Vu, M. A. Izquierdo, J. A. Bull and M. K. Kuimova, *Chem. Commun.*, 2014, **50**, 5282-5284.

13. L. Wang, Y. Xiao, W. Tian and L. Deng, *J. Am. Chem. Soc.*, 2013, **135**, 2903-2906.
14. Z. Yang, Y. He, J. H. Lee, N. Park, M. Suh, W.-S. Chae, J. Cao, X. Peng, H. Jung, C. Kang and J. S. Kim, *J. Am. Chem. Soc.*, 2013, **135**, 9181-9185.
15. E. Gatzogiannis, Z. Chen, L. Wei, R. Wombacher, Y.-T. Kao, G. Yefremov, V. W. Cornish and W. Min, *Chem. Commun.*, 2012, **48**, 8694-8696.
16. M. K. Kuimova, S. W. Botchway, A. W. Parker, M. Balaz, H. A. Collins, H. L. Anderson, K. Suhling and P. R. Ogilby, *Nature Chem.*, 2009, **1**, 69-73.
17. Y. Zhang, X. Yue, B. Kim, S. Yao and K. D. Belfield, *Chem. Eur. J.*, 2014, **20**, 7249-7253.
18. E. R. Trivedi, A. S. Harney, M. B. Olive, I. Podgorski, K. Moin, B. F. Sloane, A. G. M. Barrett, T. J. Meade and B. M. Hoffman, *Proc. Natl. Acad. Sci. U.S.A.*, 2010, **107**, 1284-1288.
19. E. R. Trivedi, B. J. Vesper, H. Weitman, B. Ehrenberg, A. G. M. Barrett, J. A. Radosevich and B. M. Hoffman, *Photochem. Photobiol.*, 2010, **86**, 410-417.
20. R. Bonnett, *Chemical aspects of Photodynamic Therapy*, Gordon and Breach Science Publishers, Amsterdam, 2000.
21. J. H. Pinthus, A. Bogaards, R. Weersink, B. C. Wilson and J. Trachtenberg, *J. Urology*, 2006, **175**, 1201-1207.
22. M. T. Jarvi, M. J. Niedre, M. S. Patterson and B. C. Wilson, *Photochem. Photobiol.*, 2006, **82**, 1198-1210.
23. B. C. Wilson and M. S. Patterson, *Phys. Med. Biol.*, 2008, **53**, R61-R109.
24. S. R. H. Davidson, R. A. Weersink, M. A. Haider, M. R. Gertner, A. Bogaards, D. Giewercer, A. Scherz, M. D. Sherar, M. Elhilali, J. L. Chin, J. Trachtenberg and B. C. Wilson, *Phys. Med. Biol.*, 2009, **54**, 2293-2313.
25. A. Gollmer, F. Besostri, T. Breitenbach and P. R. Ogilby, *Free Radical Res.*, 2013, **47**, 718-730.
26. B. W. Pedersen, T. Breitenbach, R. W. Redmond and P. R. Ogilby, *Free Radical R.*, 2010, **44**, 1383-1397.
27. F. M. Pimenta, R. L. Jensen, L. Holmegaard, T. V. Esipova, M. Westberg, T. Breitenbach and P. R. Ogilby, *J. Phys. Chem. B*, 2012, **116**, 10234-10246.
28. A. Blázquez-Castro, T. Breitenbach and P. R. Ogilby, *Photochem. Photobiol. Sci.*, 2014, **13**, 1235-1240.
29. T. Förster and G. Hoffmann, *Z. Phys. Chem. Neue Fol.*, 1971, **75**, 63-76.
30. M. A. Digman, V. R. Caiolfa, M. Zamai and E. Gratton, *Biophys. J.*, 2008, **94**, L14-L16.
31. D. M. Owen, D. J. Williamson, A. Magenau and K. Gaus, *Nat. Commun.*, 1, **3**, 1256-1258.
32. A. V. Yakimansky, T. K. Meleshko, D. M. Ilgach, M. A. Bauman, T. D. Anan'eva, L. G. Klapshina, S. A. Lermontova, I. V. Balalaeva and W. E. Douglas, *J. Polym. Sci. Part A: Polym. Chem.*, 2013, **51**, 4267-4281.
33. A. Sholto, S. Lee, B. M. Hoffman, A. G. M. Barrett and B. Ehrenberg, *Photochem. Photobiol.*, 2008, **84**, 764-773.
34. Y. Wu, M. Štefl, A. Olzyńska, M. Hof, G. Yahioglu, P. Yip, D. R. Casey, O. Ces, J. Humpolíčková and M. K. Kuimova, *Phys. Chem. Chem. Phys.*, 2013, **15**, 14986-14993.
35. K. Lang, J. Mosinger and D. M. Wagnerová, *Coord. Chem. Rev.*, 2004, **248**, 321-350.
36. R. K. Pandey and G. Zeng, *Phorphyrins as photosensitizers in photodynamic therapy*, Academic Press, New York, 2000.
37. D. E. J. G. J. Dolmans, D. Fukumura and R. K. Jain, *Nat. Rev. Cancer*, 2003, **3**, 380-387.
38. M. J. Fuchter, C. Zhong, H. Zong, B. M. Hoffman and A. G. M. Barrett, *Aust. J. Chem.*, 2008, **61**, 235.
39. M. Ethirajan, Y. Chen, P. Joshi and R. K. Pandey, *Chem. Soc. Rev.*, 2010, **40**, 340.
40. M. U. Winters, J. Kärnbratt, M. Eng, C. J. Wilson, H. L. Anderson and B. Albinsson, *J. Phys. Chem. C*, 2007, **111**, 7192-7199.
41. E. F. F. da Silva, B. W. Pedersen, T. Breitenbach, R. Toftegaard, M. K. Kuimova, L. G. Arnaut and P. R. Ogilby, *J. Phys. Chem. B*, 2012, **116**, 445-461.
42. M. K. Kuimova, G. Yahioglu and P. R. Ogilby, *J. Am. Chem. Soc.*, 2009, **131**, 332-340.

Table of contents for:

DUAL USE OF PORPHYRAZINES AS SENSITIZERS AND VISCOSITY MARKERS DURING PHOTODYNAMIC THERAPY

M. Angeles Izquierdo,[a] Aurimas Vyšniauskas,[a] Svetlana A. Lermontova,[b] Ilya S. Grigoryev,[b] Natalia Y. Shilyagina,[c] Irina V. Balalaeva,[c] Larisa G. Klapshina,[b, c *] Marina K. Kuimova[a *]

[a] Department of Chemistry, Imperial College London, Exhibition Road, London SW7 2AZ, United Kingdom

[b] Institute of Organometallic Chemistry of the RAS, Nizhny Novgorod, Russia

[c] Lobachevsky State University of Nizhny Novgorod, Nizhny Novgorod, Russia

A dual photoactive macrocycle enables simultaneous viscosity measurements and photodynamic therapy treatment, allowing the monitoring of PDT progress by FLIM